Published in final edited form as:
Neurotoxicology. 2013 September ; 38: 67–73. doi:10.1016/j.neuro.2013.06.002.

Iron depletion increases manganese uptake and potentiates apoptosis through ER stress

Young Ah Seo, **Yuan Li**, and **Marianne Wessling-Resnick***
Departments of Genetics & Complex Diseases and Nutrition, Harvard School of Public Health, Boston, MA 02115

Abstract

Iron deficiency is a risk factor for manganese (Mn) accumulation. Excess Mn promotes neurotoxicity but the mechanisms involved and whether iron depletion might affect these pathways is unknown. To study Mn intoxication *in vivo*, iron deficient and control rats were intranasally instilled with 60 mg $MnCl_2$/kg over 3 weeks. TUNEL staining of olfactory tissue revealed that Mn exposure induced apoptosis and that iron deficiency potentiated this effect. *In vitro* studies using the dopaminergic SH-SY5Y cell line confirmed that Mn-induced apoptosis was enhanced by iron depletion using the iron chelator desferrioxamine. Mn has been reported to induce apoptosis through endoplasmic reticulum stress. In SH-SY5Y cells, Mn exposure induced the ER stress genes glucose regulated protein 94 (GRP94) and C/EBP homologous protein (CHOP). Increased phosphorylation of the eukaryotic translation initiation factor 2α (phospho-eIF2α) was also observed. These effects were accompanied by the activation of ER resident enzyme caspase-12, and the downstream apoptotic effector caspase-3 was also activated. All of the Mn-induced responses were enhanced by DFO treatment. Inhibitors of ER stress and caspases significantly blocked Mn-induced apoptosis and its potentiation by DFO, indicating that ER stress and subsequent caspase activation underlie cell death. Taken together, these data reveal that Mn induces neuronal cell death through ER stress and the UPR response pathway and that this apoptotic effect is potentiated by iron deficiency most likely through upregulation of DMT1.

Keywords

DMT1; Iron deficiency; Endoplasmic reticulum; SH-SY5Y cells

1. Introduction

Manganese (Mn) is an essential nutrient required for proper development and brain function (Prohaska, 1987). In the brain, Mn is an important cofactor for the anti-oxidant enzyme superoxide dismutase, as well as enzymes involved in neurotransmitter synthesis and metabolism (Golub et al., 2005). Mn is also a potent toxicant. High levels of airborne Mn occur in occupational settings of mining, Mn ore processing, dry battery manufacture, and organochemical fungicide use (Barbeau, 1984; Donaldson, 1987). Environmental concerns

*Corresponding author: Dept. of Genetics and Complex Diseases, Harvard School of Public Health, 665 Huntington Avenue, Boston, MA 02115, Tel.: +1 617 432 3267; fax: +1 617 432 5236. wessling@hsph.harvard.edu.

Conflict of interest: The authors declare no conflicts of interest.

also have been raised by the use of a Mn-containing fuel additive, methylcyclopentadienyl manganese tricarbonyl (MMT) and the increased environmental burdens resulting from its combustion (Zayed et al., 1994; Frumkin et al., 1997). Clinical studies document that excess Mn, or manganism, results in a neurobehavioral syndrome with cognitive, psychiatric, and movement abnormalities similar to Parkinson's disease (Sriram et al., 2010). Accumulating evidence indicates detrimental effects of Mn exposure occur in children. High levels of hair Mn have been noted in learning disabled children (Pihl et al., 1977) and in hyperactive and learning disabled children (Collipp et al., 1983). High Mn in well water is associated with impaired intellectual function and hyperactive behavior in children (Bouchard et al., 2007). Children on long-term parenteral nutrition are also known to be at risk for Mn poisoning, and patient cases have been reported with movement disorders (Fell et al., 1996). Despite growing awareness of the problems associated with Mn neurotoxicity, particularly in children, little is known about the molecular mechanisms underlying Mn neurotoxicity.

Endoplasmic reticulum (ER) stress has been implicated in various neurodegenerative diseases (Imai et al., 2001; Kouroku et al., 2002; Katayama et al., 2004). ER stress triggers the unfolded protein response (UPR) to reduce protein synthesis and increase the capacity of protein folding (Kaufman, 1999). However, under prolonged ER stress, the UPR initiates signaling pathways that promote apoptosis. Thus, ER stress and UPR activation lead to cell death *via* apoptotic signaling thereby promoting neurodegeneration (Lindholm et al., 2006). It has been postulated that Mn elicits its toxic response by inducing apoptosis (Schrantz et al., 1999; Anantharam et al., 2002; Hirata, 2002; Oubrahim et al., 2002). Previous studies have shown that Mn alone promotes ER stress and causes cytotoxicity in nigral dopaminergic neuronal SN4741 cells (Chun et al., 2001) and neuroblastoma SK-N-MC cells (Yoon et al., 2011a), supporting the model that Mn-induced ER stress contributes to apoptotic signaling events in neuronal cells as a result of exposure.

Several investigators have reported that iron deficiency results in increased Mn concentrations in the brain (Chua et al., 1996; Kwik-Uribe et al., 2000; Erikson et al., 2002). Studies from our group have shown that iron deficiency anemia enhances Mn absorption across the olfactory tract to the brain (Kim et al., 2012), and using the Belgrade rat, a mechanistic role for diavalent metal transporter-1 (DMT1) in this pathway was defined (Thompson et al., 2007). DMT1 levels increase upon iron deficiency (Kelleher et al., 2004), therefore uptake of Mn can respond to low iron status. The interactions between iron deficiency and Mn exposure are particularly important because it is the most prevalent nutritional deficiency worldwide and is most common in children. A recent study in Karichi indicates that iron deficiency enhances Mn levels in children (Rahman et al., 2013). To further understand this problem, we studied mechanistic relationships between Mn toxicity and iron deficiency *in vivo* and *in vitro*.

2. Material and methods

2.1. Animals and diets

This study was conducted according to the recommendations in the Guide for the Care and Use of Laboratory Animals of the National Institutes of Health. The protocol was approved by the Harvard Medical Area Animal Care and Use Committee (Animal Experimentation Protocol AEP #04545). Weanling Sprague-Dawley rats (Taconic) were fed control (220 mg iron/kg, PicoLab 5053, PharmaServ) or iron-deficient chow (5 mg iron/kg, TD99397, Harlan Teklad) for three weeks to establish control and iron-deficient cohorts as previously described (Thompson et al., 2007). To study Mn intoxication *in vivo*, pair-fed iron-deficient and control rats were intranasally instilled with 10 mg $MnCl_2$/kg twice a week for three weeks (total of 60 mg/kg) into the right nostril with thin gel loading tips under isoflurane anesthesia. Distilled water (vehicle) was used as an instillation control. At the end of the

study, rats were euthanized by isoflurane overdose followed by exsanguination for collection of brain tissues to analyze Mn neurotoxicity.

2.2. TUNEL staining and quantitation of apoptotic cells

Brains from rats instilled with water or 60 mg $MnCl_2$/kg as described above (3–4 per group) were dissected and frozen in isopentane in a dry ice bath at −25 °C. Sections (10 μm) were cut on cryostat at −18 °C, fixed in 4% paraformaldehyde for 20 minutes and permeabilized by 10 μg/ml proteinase K for 10 minutes at room temperature. The sections were detected for apoptotic cells by terminal deoxynucleotidyl transferase-mediated dUTP nick end labeling (TUNEL) method using the In Situ Cell Death Kit, POD (Roche Diagnostics). Hematoxylin was used for counterstaining. To quantify apoptotic cells using TUNEL assay, the number of TUNEL-positive staining cells on tissue sections were divided by number of total cells at 40 x magnification using a light microscope (Carl Zeiss, Jena, Germany).

2.3. Cell culture reagents

All culture media and supplements were purchased from Invitrogen (Carlsbad, CA), except for heat-inactivated fetal bovine serum, which was purchased from Sigma (St. Louis, MO). Manganese chloride ($MnCl_2$), desferrioxamine (DFO), dimethylsulfoxide (DMSO), and ER stress inhibitor 4-phenylbutyrate (4-PBA) were purchased from Sigma (St. Louis, MO). The broad-range caspase inhibitor Z-VAD-FMK and caspase-3 inhibitor Z-DEVD-FMK were purchased from R&D Systems (Minneapolis, MN).

2.4. Cell culture and viability

Human SH-SY5Y cells were grown in DMEM containing 10% fetal bovine serum, penicillin (100 IU/ml), and streptomycin (100 μg/ml) at 37 °C in a humidified, 5% CO_2 incubator. DFO (50 uM) or vehicle control was added to the tissue culture media 24 h before addition $MnCl_2$ (0, 10, 50, 100, 500, and 1000 μM). Cell viability was assessed by the conversion of the dye 3-[4,5-dimethylthiazol-2-yl]-2,5-diphenyltetrazoliumbromide (MTT, Sigma-Aldrich) to formazan. At times indicated, cells were incubated for 4 h with MTT (5 mg/ml) and then solvent (isopropyl alcohol containing 0.1N HCl) was added to dissolve the formazan formed. The resulting formazan was quantified spectrophotometrically at 570 nm and the background was subtracted at 690 nm using a Biotek Synergy 2 plate reader (Biotek, Winooski, VT).

2.5. Immunoblot analysis

Cells were washed twice with ice-cold phosphate-buffered saline (PBS), and the total lysates were prepared in lysis buffer (50 mM Tris–HCl, 150 mM NaCl, 1 % NP-40) containing protease inhibitor cocktail (Complete Mini, Roche). Protein concentration was determined by Bradford assay. Samples (50–100 μg) were separated by electrophoresis, transferred to nitrocellulose membrane (Millipore), and immunoblotted with mouse anti-CHOP antibody (1:100, Santa Cruz), rabbit anti-GRP94 antibody (1:1,000, Santa Cruz), or phospho-eIF2α (1:1,000, Cell Signaling). Primary antibody was detected with horseradish peroxidase-conjugated IgG and proteins were visualized by enhanced chemiluminescence (SuperSignal West Pico, Pierce) following exposure to autoradiography film. The immunoblots were scanned and relative band density was determined using ImageJ (National Institutes of Health, Bethesda, MD).

2.6. Determination of caspase activity

Cell lysates were collected using NET buffer (150 mM NaCl, 5 mM EDTA, 10 mM Tris pH 7.4, and 1% Triton). Samples were then incubated with 50 μM caspase-3 substrate Ac-DMQD-AMC (Bachem, Torrance, CA) or caspase-12 substrate ATAD-AFC (Biovision,

Mountain View, CA) in reaction buffer at 37 °C for 2 hrs. The caspase-12 (excitation 400 nm - emission 510nm) and the caspase-3 (excitation 360 nm - emission 460 nm) fluorescence were measured using a Biotek Synergy 2 plate reader (Biotek, Winooski, VT). Activity was normalized to protein concentration measured by Bradford assay.

2.7. ^{54}Mn uptake assay

SH-SY5Y cells were treated with or without 50 μM DFO for 24 h. Cells were then incubated at 37°C for 20 min in assay buffer (25 mM Tris, 25 mM MES, 140 mM NaCl, 5.4 mM KCl, 1.8 mM $CaCl_2$, 0.8 mM $MgSO_4$, 5 mM glucose, pH 6.75) containing 1 μM ^{54}Mn. $^{54}MnCl_2$ (12.51 mCi/mL) was obtained from Perkin-Elmer/NEN (Boston, MA). Mn stock solution (5.6 mM) was diluted in assay buffer (25 mM Tris, 25 mM MES, 140 mM NaCl, 5.4 mM KCl, 1.8 mM $CaCl_2$, 0.8 mM $MgSO_4$, 5 mM glucose, pH 6.75) at a final $^{54}Mn^{2+}$ concentration of 1 μM. SH-SY5Y cells were treated with or without 50 μM DFO for 24 h and then incubated at 37°C for 20 min in the presence of 1 μM ^{54}Mn in assay buffer. Cells were chilled on ice and then washed three times with PBS to remove any unbound ^{54}Mn. Cell-associated radioactivity was determined in a gamma counter (Cobra Quantum, Packard Instruments, IL) and was normalized to cell protein measured in lysates by using the Bradford assay.

2.8. Statistical analysis

Results are presented as means ± SEM from at least three independent experiments. Statistical comparisons were determined using Student's *t*-test and two-way ANOVA followed by Bonferroni *post hoc* test (Prism Graph Pad, Berkeley, CA). Values of $P < 0.05$ were considered statistically significant.

3. Results

3.1. Iron deficiency potentiates Mn-induced apoptosis in rat olfactory bulb

To examine the influence of iron deficiency on Mn intoxication *in vivo*, pair-fed iron-deficient and control rats were intranasally instilled with 10 mg $MnCl_2$/kg twice weekly for a total 60 mg $MnCl_2$/kg exposure. Olfactory bulbs were collected and apoptotic cell death was assessed by terminal deoxynucleotidyltransferase dUTP nick end-labeling (TUNEL) assay. Few TUNEL-positive apoptotic cells were found in control rats intranasally instilled with water (Fig. 1A). More TUNEL-positive staining was observed in iron-deficient control rats, with even greater staining in both Mn-instilled control and Mn-instilled iron-deficient rats. These data were quantified by counting several fields from different sections for each group (at least 100 cells from each condition). The percentage of apoptotic cells in Mn-instilled rats was significantly increased compared with water-instilled control rats (Fig. 1B). Iron-deficient rats intranasally-instilled with $MnCl_2$ showed a significantly higher percentage of apoptotic cells compared with both Mn-instilled control rats and water-instilled iron-deficient rats. These data indicate that intranasal instillation of Mn induces neuronal cell death in rat olfactory bulbs and this apoptotic effect is potentiated by iron deficiency.

3.2. Mn-induced cytotoxicity is potentiated by iron depletion in vitro

To explore the molecular mechanism of Mn-induced neuronal cell apoptosis, the dopaminergic SH-SY5Y cell line was studied. Cells were treated with or without the iron chelator DFO to deplete iron for 24 h prior to addition of 0, 10, 50, 100, 500, and 1000 μM $MnCl_2$. Cell viability was measured using MTT as detailed in the Methods section. As shown in Fig. 2, Mn induced cytotoxicity was concentration dependent. DFO treatment in combination with Mn at 1 mM led to a three-fold increase ($P < 0.05$) in cytotoxicity

compared to Mn alone (Fig. 2). These data indicate that Mn-induced cell death is potentiated by iron depletion *in vitro*.

3.3. Iron depletion increases DMT1-mediated Mn uptake

Because DMT1 is known to be responsible for both Fe and Mn uptake (Shawki et al., 2012), we determined the effects of the iron chelator DFO on Mn uptake into the cells. DFO treatment significantly increased protein levels of DMT1 in SH-SY5Y cells compared to control cells (Fig. 3A). To verify the effect of DFO on DMT1-mediated transport activity, we measured ^{54}Mn uptake into the cells. DFO-treated cells took up ~70% more ^{54}Mn compared to control cells (Fig. 3B). Taken together, these data indicate that iron depletion by DFO leads to increased levels of DMT1, thereby enhancing transport of Mn into cells.

3.4. Mn induces the ER stress response and caspase activation and these effects are enhanced by iron depletion

ER stress is thought to induce cell death *via* apoptotic signaling (Katayama et al., 2004; Vitte et al., 2010). Accordingly, we examined the effect of Mn treatment on ER stress responses and caspase activation. A significant increase in levels of ER stress response proteins was observed after 9 h of Mn exposure, including induction of the ER chaperone GRP94 and the pro-apoptotic GADD153/CHOP protein (Fig. 4A). Phosphorylation of eIF2α, a known UPR signaling response, was also enhanced (Fig. 4B). These data suggest that Mn-induced apoptotic cell death is, at least in part, mediated through ER stress. Moreover, treatment with DFO further enhanced the levels of GRP94 and GADD153/CHOP in the presence of Mn.

The ER-resident cysteine protease caspase-12 is activated during ER stress-induced apoptotic signaling (Yoneda et al., 2001; Breckenridge et al., 2003). Thus, we next determined whether Mn induces caspase-12 activity and the effect of iron depletion on this process. Caspase-12 activity was determined using a fluorometric assay that detects specific enzymatic cleavage of the substrate ATAD-AFC by the release of fluorescent product. Caspase-12 activity increased in a time-dependent manner in SH-SY5Y cells treated with Mn, and this substrate cleavage was enhanced by DFO (Fig. 4C). We also tested whether activation of the initiator caspase-12 would lead to activation of proapoptotic effector caspase-3. Caspase-3 activity was again assessed using a fluorometric assay, in this case monitoring cleavage of the caspase-3 specific substrate Ac-DEVD-AMC. As shown in Fig. 5, cells treated with DFO and Mn displayed increased caspase-3 activity with a significant Fe x Mn effect ($P = 0.016$).

3.6. Inhibition of caspase activity and ER stress provides neuroprotection

To further elucidate the role of Mn-induced apoptotic signaling pathways in neuronal cell death, we investigated the effect of pan-caspase inhibitior (Z-VAD-FMK), caspase-3 inhibitor (Z-DEVD-FMK), and ER stress inhibitor (4-PBA) on cytotoxicity. Caspase inhibition reversed SH-SY5Y cell death induced by Mn (Fig. 6A), suggesting that caspase-3 and possibly other caspase activities like caspase-12 play a pivotal role in Mn cytotoxicity. Furthermore, inhibition of ER stress by the chemical chaperone 4-PBA completely blocked SH-SY5Y cell death both in the absence or presence of DFO (Fig. 6B). This evidence indicates that iron depletion by DFO acts to enhance ER stress-mediated apoptotic signaling by Mn.

4. Discussion

Chronic Mn exposure is common in occupational settings of mining, Mn ore processing, dry battery manufacture, and organochemical fungicide use (Barbeau, 1984; Donaldson, 1987).

Severe neurotoxic consequences of Mn exposure are displayed in “manganism” and are similar to Parkinson’s disease (Sriram et al., 2010). Increasing evidence suggests lower levels of Mn may also induce behavioral deficits. Luccini and his co-workers showed that a group of Italian ferroalloy workers who had been exposed to low levels of Mn dust by inhalation exhibited neruofunctional changes (Lucchini et al., 1999). More recent studies have shown that long-term exposures to low levels of anthropogenic or environmental sources of Mn induced deficits in motor function in non-human primates (Guilarte et al., 2006). The major route for Mn exposure on health effects is through inhalation. DMT1 is not only the major transporter for iron absorption in the duodenum (Gunshin et al., 1997; Fleming et al., 1998), but also mediates uptake of Mn across the olfactory epithelium into the brain (Thompson et al., 2007). Iron deficiency upregulates the expression of DMT1 in both olfactory and intestinal epithelia (Gunshin et al., 1997; Canonne-Hergaux et al., 1999; Thompson et al., 2007), and upregulation of DMT1 in iron-deficient rats is associated with increased Mn uptake into the brain (Thompson et al., 2007).

The substania nigra and globus pallidus are known to accumulate Mn and motor deficits due to neurodegeneration in these areas are associated with Parkinson’s Disease and manganism (Baek et al., 2003). The olfactory bulb is another brain area that accumulates Mn (Donaldson et al., 1973; Bonilla et al., 1982). Metal workers exposed to welding fumes have olfactory dysfunction, and Parkinson’s disease patients also display similar loss of function (Antunes et al., 2007; Doty, 2012). Our *in vivo* study of rats intranasally instilled with Mn reveals that olfactory exposure promotes apoptosis of olfactory neurons and that iron deficiency enhances this effect. These observations suggest the underlying basis for olfactory dysfunction due to Mn exposure arises due to cell death, and further suggest these deficits might be potentiated in iron-deficient individuals.

Mn is known to induce apoptosis (Schrantz et al., 1999; Anantharam et al., 2002; Hirata, 2002; Oubrahim et al., 2002) through ER stress (Chun et al., 2001; Yoon et al., 2011a). We investigated Mn cytotoxicity in dopaminergic SH-SY5Y cells, an *in vitro* model previously used to study neurodegenerative processes and neurotoxicity, as well as manganism and Parkinson’s disease (Higashi et al., 2004; Shang et al., 2005). Our *in vitro* studies confirm that Mn induces cell death. As shown by others (Roth et al., 2003; Hirata et al., 2004; Stredrick et al., 2004; Latchoumycandane et al., 2005), relatively high concentrations of Mn were required to recapitulate cytotoxic effects in cell culture studies (>500 μM). It should be noted that the divalent cation is bound by serum proteins present in culture media and the actual free metal concentrations are considerably lower. This idea is supported by increased sensitivity to the divalent metals as serum concentrations in the media are reduced (Lin et al., 1993). For example, Stephson et al (Stephenson et al., 2013) determined an LD_{50} value of 12.98 μM Mn^{2+} for SH-SY5Y cells under reduced serum (2% FBS). SH-SY5Y cell experiments in our study were carried out with 10% FBS, and therefore Mn concentrations observed to induce cell death are more consistent with those reported in studies using similar conditions with other neuronal cell lines (Hirata, 2002; Yoon et al., 2011a; Yoon et al., 2011b).

Importantly, iron depletion by DFO treatment enhanced Mn-induced cytotoxicity in SH-SY5Y cells. Previous studies in astrocytes have shown that DFO enhances Mn uptake through DMT1 (Erikson and Aschner, 2006). In contrast, iron deficiency promoted by high copper treatment of astrocytes did not affect Mn uptake (Scheiber et al., 2010; Qian et al., 2012). It is clear that interactions between metals like copper, iron and manganese play a critical role in cell homeostasis. Our study is the first to investigate how iron deficiency influences Mn transport and toxicity in neuronal cells. We suggest that upregulation of DMT1 in neuronal cells leads to increased intracellular Mn, potentiating the effective LD_{50}. These results predict that iron-responsive Mn transport into the brain *via* DMT1 leads to Mn

accumulation into neuronal cells, to promote neurotoxic effects of Mn in iron-deficient rats. Given the role of astrocytes in Mn-mediated neurotoxicity (Sidoryk-Wegrzynowicz et al., 2013), iron-responsive changes in Mn levels in this cell type might compound these effects. Overall, these findings generally imply that low body iron status contributes to enhanced susceptibility of neurons to Mn toxicity. This problem might be particularly acute in children who are most vulnerable to iron deficiency (Pihl et al., 1977; Collipp et al., 1983; Bouchard et al., 2007).

Our study further explores how Mn interacts with iron to induce neurotoxicity at the molecular level. ER stress-mediated apoptotic signalling contributes to the pathogenesis of neurodegenerative diseases (Katayama et al., 2004; Vitte et al., 2010), and many studies have indicated a link to Mn toxicity as indicated above. The ER is a multifunctional signaling organelle that controls a wide range of cellular processes (Berridge, 2002). The accumulation of unfolded proteins within the ER induces ER stress and triggers a coordinated adaptive program called UPR. The UPR alleviates ER stress by decreasing protein synthesis and upregulating both the protein folding and the degradation pathways, leading to cellular recovery (Mori, 2000; Shen et al., 2004). Under prolonged ER stress, the UPR initiates signaling pathways that promote apoptosis. The molecular chaperone GRP94 and pro-apoptotic protein CHOP are the major components of the ER stess-mediated apoptotic signaling pathways. These ER stress response genes are markedly induced in response to ER dysfunction (Lee, 2001) and thus widely used as markers for ER stress. In addition, the activation of caspase-12 in response to ER stress has been suggested as a putative molecular marker for apoptosis (Yoneda et al., 2001; Breckenridge et al., 2003). In the present study, we showed that Mn induced ER stress as indicated by the increased protein levels of GRP94 and CHOP and increased activity of caspase-12. Suppression of ER stress by the chemical chaperone 4-PBA fully reversed Mn-induced cytotoxicity, indicating that inhibition of ER stress may provide protective effects on neuronal cells against Mn toxicity. Further studies will be required to test whether these neuroprotective effects by inhibiting ER stress will occur in *in vivo* models of Mn neurotoxicity.

Our data indicate that iron depletion by DFO potentiates these Mn-induced ER stress responses and apoptosis by increasing levels of Mn present in neuronal cells. Other possible mechanisms contributing to this effect include cell cycle arrest and/or apoptosis caused by hypoxia or nutrient deprivation (Carlson et al., 1993; Abcouwer et al., 1999; Fanzo et al., 2001). Recent studies focused on the growth arrest and DNA damage reported that iron chelation increased expression of GADD153/CHOP gene (Darnell et al., 1999). Similar to effects we observed with iron depletion, hypoxia upregulates the expression of GADD153/CHOP gene (Price et al., 1992). Thus, it is conceivable that Mn-induced GADD153/CHOP expression is enhanced by iron depletion by other indirect mechansims unrelated to upregulated Mn transport. In addition, other eIF2α kinases may sense stress exerted through iron deficiency. These eIF2α kinases include GCN2, which is activated by nutritional deprivation, and HRI, which links protein synthesis to heme availability in erythroid cells and is also activated by heme deficiency and oxidative stress (Wek et al., 2007; Sonenberg et al., 2009). All three UPR signaling pathways can regulate CHOP-mediated apoptosis of neurons (Shkoda et al., 2007) and that activation of the UPR signaling pathways occur by interconnected rather than independent processes to induce apoptosis.

The interaction between Mn neurotoxicity and iron deficiency may have profound implications with regard to the potential toxicity of divalent metals. While it is known that Mn induces apoptosis, the role of ER stress and caspase activation has not been fully determined. The ultimate goal is to learn how the metal engages this important cellular process to respond to the environment. While it is known that iron deficiency modifies Mn toxicity, our data indicate these effects are mediated through the ER stress response

pathway, providing new information about the molecular basis for interactions between the two metals. These studies provide insight into mechanisms of Mn neurotoxicity and raise awareness of the potential susceptibility of iron-deficient populations exposed to high Mn.

Acknowledgments

We thank Dr. Jonghan Kim for help in Mn instillation studies. This study was supported by an NIH grant through NIEHS (R01 ES0146380 and in part by Pilot Feasability Project funding from the HSPH-NIEHS Center for Environmental Health (ES000002).

References

Abcouwer SF, Schwarz C, Meguid RA. Glutamine deprivation induces the expression of GADD45 and GADD153 primarily by mRNA stabilization. J Biol Chem. 1999; 274:28645–51. [PubMed: 10497233]

Anantharam V, Kitazawa M, Wagner J, Kaul S, Kanthasamy AG. Caspase-3-dependent proteolytic cleavage of protein kinase Cdelta is essential for oxidative stress-mediated dopaminergic cell death after exposure to methylcyclopentadienyl manganese tricarbonyl. J Neurosci. 2002; 22:1738–51. [PubMed: 11880503]

Antunes MB, Bowler R, Doty RL. San Francisco/Oakland Bay Bridge Welder Study: olfactory function. Neurology. 2007; 69:1278–84. [PubMed: 17875916]

Baek SY, Lee MJ, Jung HS, Kim HJ, Lee CR, Yoo C, et al. Effect of manganese exposure on MPTP neurotoxicities. Neurotoxicology. 2003; 24:657–65. [PubMed: 12900079]

Barbeau A. Manganese and extrapyramidal disorders (a critical review and tribute to Dr. George C Cotzias). Neurotoxicology. 1984; 5:13–35. [PubMed: 6538948]

Berridge MJ. The endoplasmic reticulum: a multifunctional signaling organelle. Cell Calcium. 2002; 32:235–49. [PubMed: 12543086]

Bonilla E, Salazar E, Villasmil JJ, Villalobos R. The regional distribution of manganese in the normal human brain. Neurochem Res. 1982; 7:221–7. [PubMed: 7121709]

Bouchard M, Laforest F, Vandelac L, Bellinger D, Mergler D. Hair manganese and hyperactive behaviors: pilot study of school-age children exposed through tap water. Environ Health Perspect. 2007; 115:122–7. [PubMed: 17366831]

Breckenridge DG, Stojanovic M, Marcellus RC, Shore GC. Caspase cleavage product of BAP31 induces mitochondrial fission through endoplasmic reticulum calcium signals, enhancing cytochrome c release to the cytosol. J Cell Biol. 2003; 160:1115–27. [PubMed: 12668660]

Canonne-Hergaux F, Gruenheid S, Ponka P, Gros P. Cellular and subcellular localization of the Nramp2 iron transporter in the intestinal brush border and regulation by dietary iron. Blood. 1999; 93:4406–17. [PubMed: 10361139]

Carlson SG, Fawcett TW, Bartlett JD, Bernier M, Holbrook NJ. Regulation of the C/EBP-related gene gadd153 by glucose deprivation. Mol Cell Biol. 1993; 13:4736–44. [PubMed: 8336711]

Chua AC, Morgan EH. Effects of iron deficiency and iron overload on manganese uptake and deposition in the brain and other organs of the rat. Biol Trace Elem Res. 1996; 55:39–54. [PubMed: 8971353]

Chun HS, Lee H, Son JH. Manganese induces endoplasmic reticulum (ER) stress and activates multiple caspases in nigral dopaminergic neuronal cells, SN4741. Neurosci Lett. 2001; 316:5–8. [PubMed: 11720765]

Collipp PJ, Chen SY, Maitinsky S. Manganese in infant formulas and learning disability. Ann Nutr Metab. 1983; 27:488–94. [PubMed: 6651226]

Darnell G, Richardson DR. The potential of iron chelators of the pyridoxal isonicotinoyl hydrazone class as effective antiproliferative agents III: the effect of the ligands on molecular targets involved in proliferation. Blood. 1999; 94:781–92. [PubMed: 10397746]

Donaldson J. The physiopathologic significance of manganese in brain: its relation to schizophrenia and neurodegenerative disorders. Neurotoxicology. 1987; 8:451–62. [PubMed: 3309736]

Donaldson J, Pierre TS, Minnich JL, Barbeau A. Determination of Na +, K +, Mg 2+, Cu 2+, Zn 2+, and Mn 2+ in rat brain regions. Can J Biochem. 1973; 51:87–92. [PubMed: 4689096]

Doty RL. Olfactory dysfunction in Parkinson disease. Nat Rev Neurol. 2012; 8:329–39. [PubMed: 22584158]

Erikson KM, Shihabi ZK, Aschner JL, Aschner M. Manganese accumulates in iron-deficient rat brain regions in a heterogeneous fashion and is associated with neurochemical alterations. Biol Trace Elem Res. 2002; 87:143–56. [PubMed: 12117224]

Fanzo JC, Reaves SK, Cui L, Zhu L, Wu JY, Wang YR, et al. Zinc status affects p53, gadd45, and c-fos expression and caspase-3 activity in human bronchial epithelial cells. Am J Physiol Cell Physiol. 2001; 281:C751–7. [PubMed: 11502552]

Fell JM, Reynolds AP, Meadows N, Khan K, Long SG, Quaghebeur G, et al. Manganese toxicity in children receiving long-term parenteral nutrition. Lancet. 1996; 347:1218–21. [PubMed: 8622451]

Fleming MD, Romano MA, Su MA, Garrick LM, Garrick MD, Andrews NC. Nramp2 is mutated in the anemic Belgrade (b) rat: evidence of a role for Nramp2 in endosomal iron transport. Proc Natl Acad Sci U S A. 1998; 95:1148–53. [PubMed: 9448300]

Frumkin H, Solomon G. Manganese in the U.S gasoline supply. Am J Ind Med. 1997; 31:107–15. [PubMed: 8986262]

Golub MS, Hogrefe CE, Germann SL, Tran TT, Beard JL, Crinella FM, et al. Neurobehavioral evaluation of rhesus monkey infants fed cow's milk formula, soy formula, or soy formula with added manganese. Neurotoxicol Teratol. 2005; 27:615–27. [PubMed: 15955660]

Guilarte TR, Chen MK, McGlothan JL, Verina T, Wong DF, Zhou Y, et al. Nigrostriatal dopamine system dysfunction and subtle motor deficits in manganese-exposed non-human primates. Exp Neurol. 2006; 202:381–90. [PubMed: 16925997]

Gunshin H, Mackenzie B, Berger UV, Gunshin Y, Romero MF, Boron WF, et al. Cloning and characterization of a mammalian proton-coupled metal-ion transporter. Nature. 1997; 388:482–8. [PubMed: 9242408]

Higashi Y, Asanuma M, Miyazaki I, Hattori N, Mizuno Y, Ogawa N. Parkin attenuates manganese-induced dopaminergic cell death. J Neurochem. 2004; 89:1490–7. [PubMed: 15189352]

Hirata Y. Manganese-induced apoptosis in PC12 cells. Neurotoxicol Teratol. 2002; 24:639–53. [PubMed: 12200195]

Hirata Y, Furuta K, Miyazaki S, Suzuki M, Kiuchi K. Anti-apoptotic and pro-apoptotic effect of NEPP11 on manganese-induced apoptosis and JNK pathway activation in PC12 cells. Brain Res. 2004; 1021:241–7. [PubMed: 15342272]

Imai Y, Soda M, Inoue H, Hattori N, Mizuno Y, Takahashi R. An unfolded putative transmembrane polypeptide, which can lead to endoplasmic reticulum stress, is a substrate of Parkin. Cell. 2001; 105:891–902. [PubMed: 11439185]

Katayama T, Imaizumi K, Manabe T, Hitomi J, Kudo T, Tohyama M. Induction of neuronal death by ER stress in Alzheimer's disease. J Chem Neuroanat. 2004; 28:67–78. [PubMed: 15363492]

Kaufman RJ. Stress signaling from the lumen of the endoplasmic reticulum: coordination of gene transcriptional and translational controls. Genes Dev. 1999; 13:1211–33. [PubMed: 10346810]

Kelleher T, Ryan E, Barrett S, Sweeney M, Byrnes V, O'Keane C, et al. Increased DMT1 but not IREG1 or HFE mRNA following iron depletion therapy in hereditary haemochromatosis. Gut. 2004; 53:1174–9. [PubMed: 15247188]

Kim J, Li Y, Buckett PD, Bohlke M, Thompson KJ, Takahashi M, et al. Iron-responsive olfactory uptake of manganese improves motor function deficits associated with iron deficiency. PLoS One. 2012; 7:e33533. [PubMed: 22479410]

Kouroku Y, Fujita E, Jimbo A, Kikuchi T, Yamagata T, Momoi MY, et al. Polyglutamine aggregates stimulate ER stress signals and caspase-12 activation. Hum Mol Genet. 2002; 11:1505–15. [PubMed: 12045204]

Kwik-Uribe CL, Golub MS, Keen CL. Chronic marginal iron intakes during early development in mice alter brain iron concentrations and behavior despite postnatal iron supplementation. J Nutr. 2000; 130:2040–8. [PubMed: 10917923]

Latchoumycandane C, Anantharam V, Kitazawa M, Yang Y, Kanthasamy A, Kanthasamy AG. Protein kinase Cdelta is a key downstream mediator of manganese-induced apoptosis in dopaminergic neuronal cells. J Pharmacol Exp Ther. 2005; 313:46–55. [PubMed: 15608081]

Lee AS. The glucose-regulated proteins: stress induction and clinical applications. Trends Biochem Sci. 2001; 26:504–10. [PubMed: 11504627]

Lin WH, Higgins D, Pacheco M, Aletta J, Perini S, Marcucci KA, et al. Manganese induces spreading and process outgrowth in rat pheochromocytoma (PC12) cells. J Neurosci Res. 1993; 34:546–61. [PubMed: 8386776]

Lindholm D, Wootz H, Korhonen L. ER stress and neurodegenerative diseases. Cell Death Differ. 2006; 13:385–92. [PubMed: 16397584]

Lucchini R, Apostoli P, Perrone C, Placidi D, Albini E, Migliorati P, et al. Long-term exposure to “low levels” of manganese oxides and neurofunctional changes in ferroalloy workers. Neurotoxicology. 1999; 20:287–97. [PubMed: 10385891]

Mori K. Tripartite management of unfolded proteins in the endoplasmic reticulum. Cell. 2000; 101:451–4. [PubMed: 10850487]

Oubrahim H, Chock PB, Stadtman ER. Manganese(II) induces apoptotic cell death in NIH3T3 cells via a caspase-12-dependent pathway. J Biol Chem. 2002; 277:20135–8. [PubMed: 11964391]

Pihl RO, Parkes M. Hair element content in learning disabled children. Science. 1977; 198:204–6. [PubMed: 905825]

Price BD, Calderwood SK. Gadd45 and Gadd153 messenger RNA levels are increased during hypoxia and after exposure of cells to agents which elevate the levels of the glucose-regulated proteins. Cancer Res. 1992; 52:3814–7. [PubMed: 1617653]

Prohaska JR. Functions of trace elements in brain metabolism. Physiol Rev. 1987; 67:858–901. [PubMed: 3299411]

Qian Y, Zheng Y, Taylor R, Tiffany-Castiglioni E. Involvement of the molecular chaperone Hspa5 in copper homeostasis in astrocytes. Brain Res. 2012; 1447:9–19. [PubMed: 22342161]

Rahman MA, Rahman B, Ahmed N. High blood manganese in iron-deficient children in Karachi. Public Health Nutr. 2013:1–7.

Roth JA, Garrick MD. Iron interactions and other biological reactions mediating the physiological and toxic actions of manganese. Biochem Pharmacol. 2003; 66:1–13. [PubMed: 12818360]

Scheiber IF, Schmidt MM, Dringen R. Zinc prevents the copper-induced damage of cultured astrocytes. Neurochem Int. 2010; 57:314–22. [PubMed: 20600438]

Schrantz N, Blanchard DA, Mitenne F, Auffredou MT, Vazquez A, Leca G. Manganese induces apoptosis of human B cells: caspase-dependent cell death blocked by bcl-2. Cell Death Differ. 1999; 6:445–53. [PubMed: 10381635]

Shang T, Kotamraju S, Zhao H, Kalivendi SV, Hillard CJ, Kalyanaraman B. Sepiapterin attenuates 1-methyl-4-phenylpyridinium-induced apoptosis in neuroblastoma cells transfected with neuronal NOS: role of tetrahydrobiopterin, nitric oxide, and proteasome activation. Free Radic Biol Med. 2005; 39:1059–74. [PubMed: 16198233]

Shawki A, Knight PB, Maliken BD, Niespodzany EJ, Mackenzie B. H(+)-coupled divalent metal-ion transporter-1: functional properties, physiological roles and therapeutics. Curr Top Membr. 2012; 70:169–214. [PubMed: 23177986]

Shen X, Zhang K, Kaufman RJ. The unfolded protein response--a stress signaling pathway of the endoplasmic reticulum. J Chem Neuroanat. 2004; 28:79–92. [PubMed: 15363493]

Shkoda A, Ruiz PA, Daniel H, Kim SC, Rogler G, Sartor RB, et al. Interleukin-10 blocked endoplasmic reticulum stress in intestinal epithelial cells: impact on chronic inflammation. Gastroenterology. 2007; 132:190–207. [PubMed: 17241871]

Sidoryk-Wegrzynowicz M, Aschner M. Role of astrocytes in manganese mediated neurotoxicity. BMC Pharmacol Toxicol. 2013; 14:23. [PubMed: 23594835]

Sonenberg N, Hinnebusch AG. Regulation of translation initiation in eukaryotes: mechanisms and biological targets. Cell. 2009; 136:731–45. [PubMed: 19239892]

Sriram K, Lin GX, Jefferson AM, Roberts JR, Chapman RS, Chen BT, et al. Dopaminergic neurotoxicity following pulmonary exposure to manganese-containing welding fumes. Arch Toxicol. 2010; 84:521–40. [PubMed: 20224926]

Stephenson AP, Schneider JA, Nelson BC, Atha DH, Jain A, Soliman KF, et al. Manganese-induced oxidative DNA damage in neuronal SH-SY5Y cells: attenuation of thymine base lesions by glutathione and N-acetylcysteine. Toxicol Lett. 2013; 218:299–307. [PubMed: 23296100]

Stredrick DL, Stokes AH, Worst TJ, Freeman WM, Johnson EA, Lash LH, et al. Manganese-induced cytotoxicity in dopamine-producing cells. Neurotoxicology. 2004; 25:543–53. [PubMed: 15183009]

Thompson K, Molina RM, Donaghey T, Schwob JE, Brain JD, Wessling-Resnick M. Olfactory uptake of manganese requires DMT1 and is enhanced by anemia. FASEB J. 2007; 21:223–30. [PubMed: 17116743]

Vitte J, Traver S, Maues De Paula A, Lesage S, Rovelli G, Corti O, et al. Leucine-rich repeat kinase 2 is associated with the endoplasmic reticulum in dopaminergic neurons and accumulates in the core of Lewy bodies in Parkinson disease. J Neuropathol Exp Neurol. 2010; 69:959–72. [PubMed: 20720502]

Wek RC, Cavener DR. Translational control and the unfolded protein response. Antioxid Redox Signal. 2007; 9:2357–71. [PubMed: 17760508]

Yoneda T, Imaizumi K, Oono K, Yui D, Gomi F, Katayama T, et al. Activation of caspase-12, an endoplastic reticulum (ER) resident caspase, through tumor necrosis factor receptor-associated factor 2-dependent mechanism in response to the ER stress. J Biol Chem. 2001; 276:13935–40. [PubMed: 11278723]

Yoon H, Kim DS, Lee GH, Kim KW, Kim HR, Chae HJ. Apoptosis Induced by Manganese on Neuronal SK-N-MC Cell Line: Endoplasmic Reticulum (ER) Stress and Mitochondria Dysfunction. Environ Health Toxicol. 2011a; 26:e2011017. [PubMed: 22232721]

Yoon H, Lee GH, Kim DS, Kim KW, Kim HR, Chae HJ. The effects of 3, 4 or 5 amino salicylic acids on manganese-induced neuronal death: ER stress and mitochondrial complexes. Toxicol In Vitro. 2011b; 25:1259–68. [PubMed: 21477646]

Zayed J, Gerin M, Loranger S, Sierra P, Begin D, Kennedy G. Occupational and environmental exposure of garage workers and taxi drivers to airborne manganese arising from the use of methylcyclopentadienyl manganese tricarbonyl in unleaded gasoline. Am Ind Hyg Assoc J. 1994; 55:53–8. [PubMed: 8116528]

Highlights

- Diet-induced iron deficiency potentiated Mn-induced neuronal apoptotic cell death in rat brain.
- Mn induced cell cytotoxicity was potentiated by iron depletion.
- Iron depletion by DFO increased DMT1-mediated Mn uptake.
- Iron depletion enhanced Mn-induced ER stress genes and activation of caspase-12 and -3.
- Inhibition of caspase activity and ER stress provides neuroprotection.

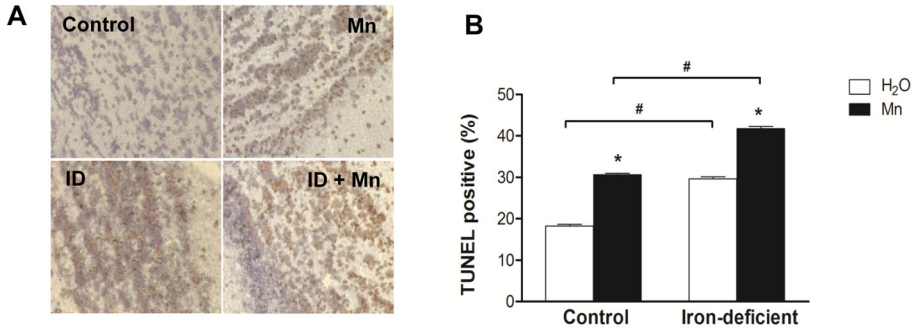

Fig. 1.

Diet-induced iron deficiency potentiated Mn-induced neuronal apoptotic cell death in rat brain. To study Mn intoxication *in vivo*, pair-fed iron-deficient and control rats were intranasally instilled with 60 mg $MnCl_2$/kg for 3 weeks. (A) Representative TUNEL staining of the olfactory bulbs in water-instilled (control), $MnCl_2$-instilled (Mn), water-instilled iron-deficient (ID), and $MnCl_2$-instilled iron-deficient (ID+Mn) rats. (B) Quantification of the percentage (%) of TUNEL-positive cells within the total number of cells. Empty and closed bars represent water-instilled and $MnCl_2$-instilled rats, respectively. Data represent as mean ± SEM (n = 3–4 samples/group). $^{*}P < 0.05$ *vs.* water-instilled group, and $^{\#}P < 0.05$ for control *vs.* iron-deficient group; two-way ANOVA.

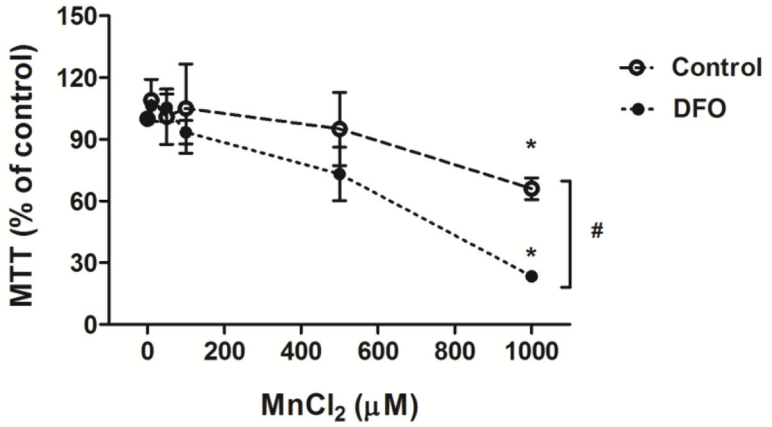

Fig. 2.

Mn induced cell cytotoxicity in SH-SY5Y cells which was potentiated by iron depletion. To assess effect of iron depletion on Mn-induced cell cytotoxicity, cells were treated with (solid circle) or without (open circle) 50 μM DFO for 24 h, followed by treatment with indicated concentrations (0, 10, 50, 100, 500, and 1000 μM) of $MnCl_2$ for another 48 h. Cell viability was measured using MTT assay. Data represent mean ± SEM as percent of values observed in untreated cells (% of control, n = 3–4 samples/treatment). $^{*}P < 0.05$ *vs.* Mn-untreated control, $^{\#}P < 0.05$ for control *vs.* DFO treatment group; two-way ANOVA.

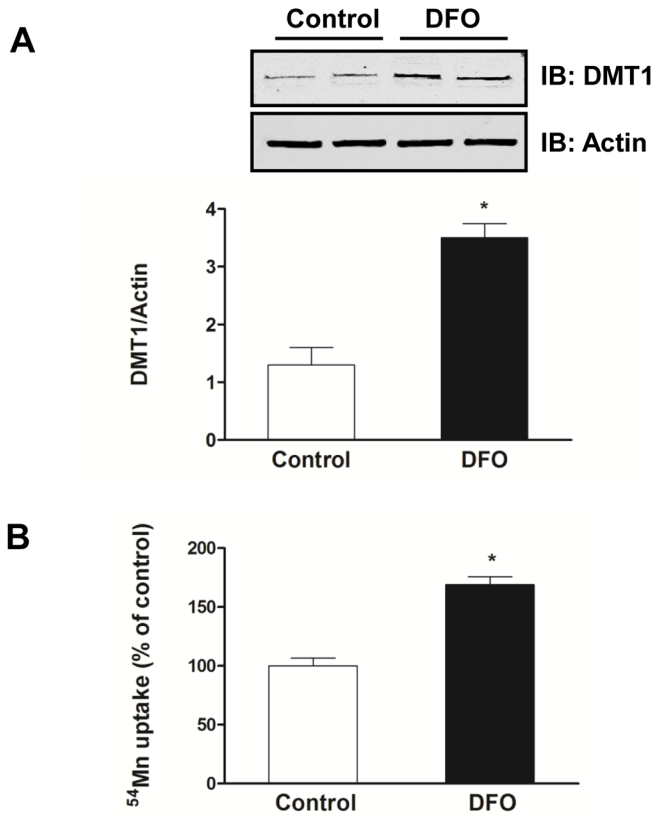

Fig. 3.

Iron depletion by DFO increased DMT1-mediated Mn uptake. (A) Representative immunoblot of DMT1 in total membrane proteins isolated from SH-SY5Y cells treated with 50 μM DFO for 24 h compared with untreated cells (Control). Equal loading was verified by immunoblotting with actin antibody. Band intensity of DMT1 was normalized to actin and expressed as relative intensity of untreated cells. Data represent mean ± SEM from two independent experiments. * $P < 0.05$ between control *vs.* DFO treatment group; student's *t*-test. (B) SH-SY5Y cells were treated with 50 μM DFO for 24 h and then incubated at 37°C for 20 min in the presence of 1 μM ^{54}Mn. Cells were chilled on ice, and washed with ice cold PBS, and cell-associated radioactivity was determined by gamma counting and normalized to control (vehicle alone). Shown are means ± SEM from at least two independent experiments (n=3). * $P < 0.05$ between control *vs.* DFO treatment group; two-way ANOVA.

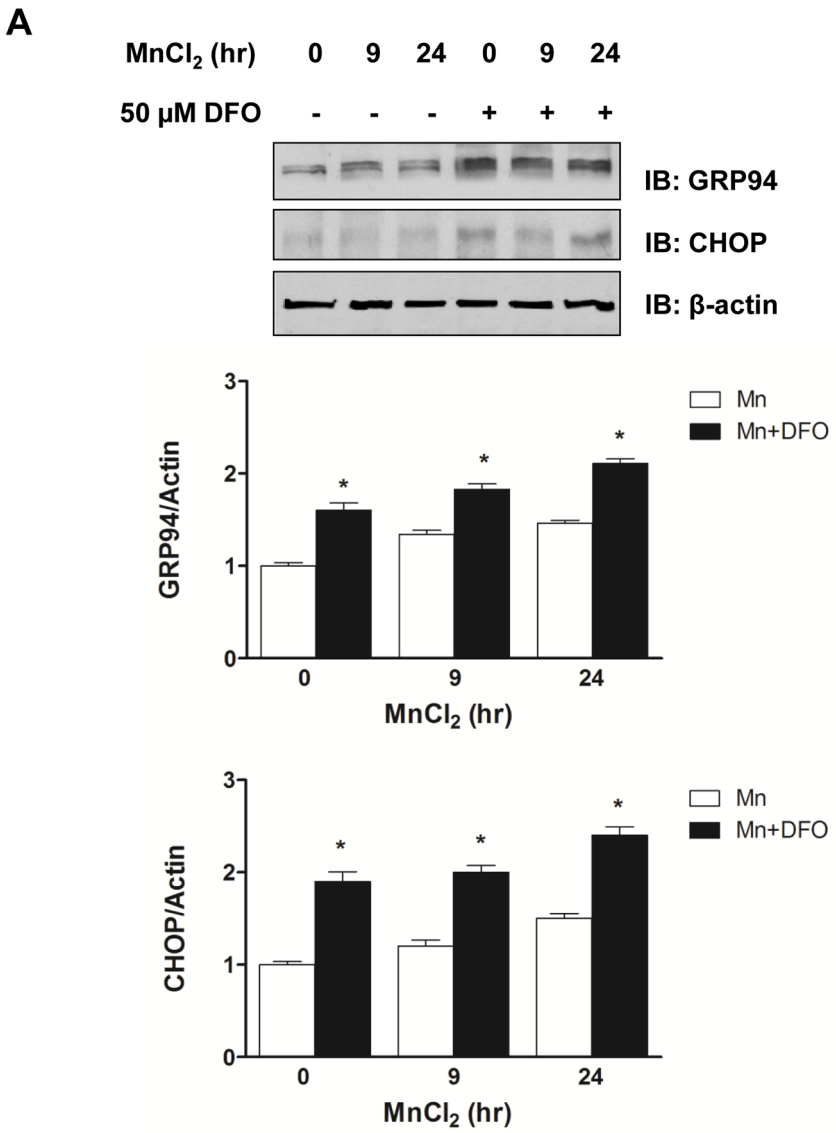

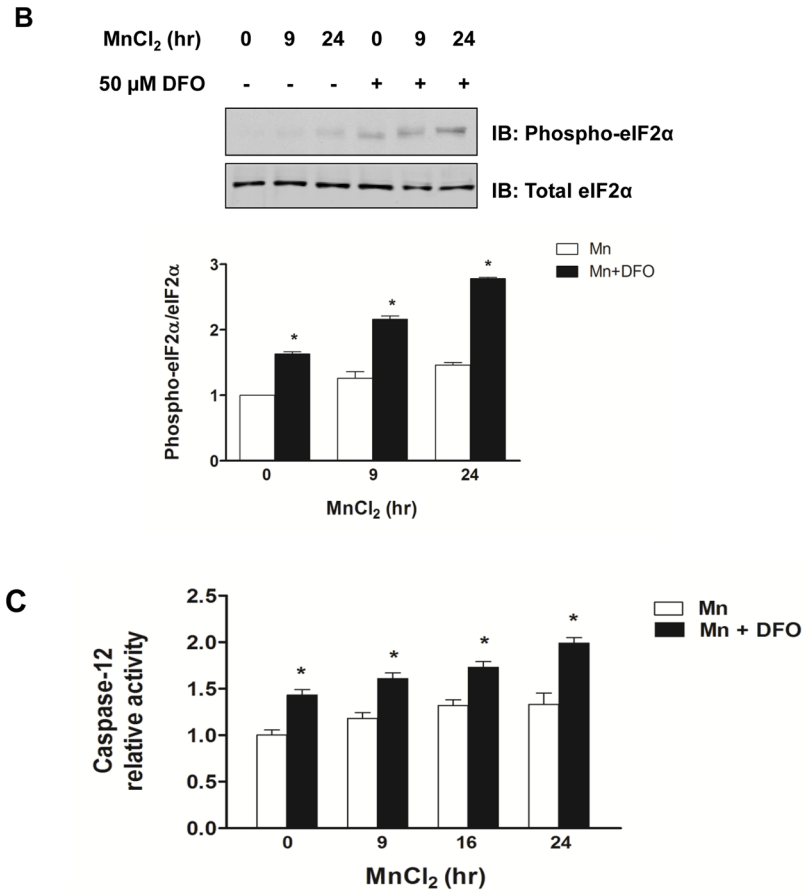

Fig. 4.

Iron depletion enhanced Mn-induced ER stress genes and activation of caspase-12. (A) Representative immunoblot of GRP94 and CHOP in SH-SY5Y cells treated with (+) or without (−) DFO before treatment of $MnCl_2$ for 9 h or 24 h. Total cell lysates were separated by SDS-PAGE, and membranes were immunoblotted with GRP94 or CHOP antibody. Band intensity of GRP94 or CHOP was normalized to actin and expressed as relative intensity of untreated cells. Data represent mean ± SEM from three independent experiments. * $P < 0.05$ *vs.* Mn treatment group; two-way ANOVA. (B) Representative immunoblot of phosphorylated eIF2α (Phospho-eIF2α) in SH-SY5Y cells treated with (+) or without (−) DFO before treatment of $MnCl_2$ for 9 h or 24 h. Total eIF2α was used as a loading control. Band intensity of P-eIF2α was normalized to eIF2α and expressed as relative intensity of untreated cells. Data represent mean ± SEM from three independent experiments. * $P < 0.05$ *vs.* Mn treatment group. (C) The caspase-12 activity in the cell lysates was determined using the fluorometric specific substrate ATAD-AFC. Fluorescence was measured in a 96-well black plate at excitation 400 nm and emission 505 nm using a microplate reader. Empty and closed bars represent $MnCl_2$-treated cells without and with DFO, respectively. Data represent mean ± SEM of relative activity observed in untreated cells (n=3 samples/ treatment). * $P < 0.05$ *vs.* Mn treatment group; two-way ANOVA.

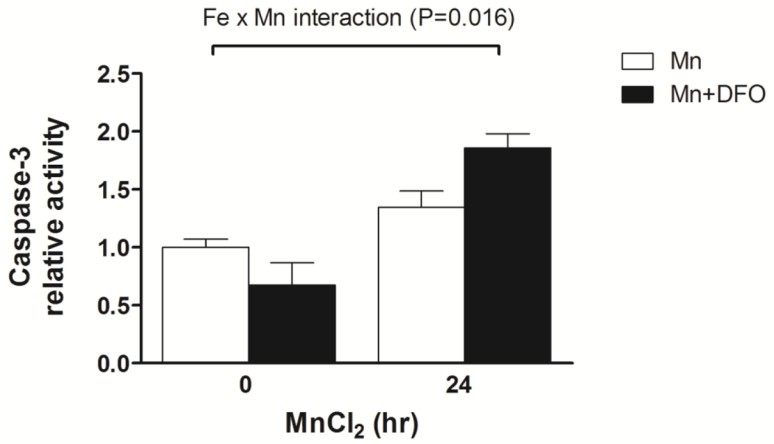

Fig. 5.

Iron depletion enhanced Mn-induced activation of caspase-3. To determine the activation of caspase-3 during Mn-induced cell cytotoxicity, cells were treated with or without 50 μM DFO for 24 h and then treated with $MnCl_2$ for 24 h. The caspase-3 activity in the cell lysates was determined using the fluorometric specific substrate Ac-DMQD-AMC. Fluorescence was measured in a 384-well black plate at excitation 360 nm and emission 460 nm using a microploate reader. Empty and closed bars represent $MnCl_2$-treated cells without and with DFO, respectively. Data represent mean ± SEM of relative activity observed in untreated cells (n = 3–6/treatment). * $P < 0.05$ *vs.* Mn treatment group; two-way ANOVA.

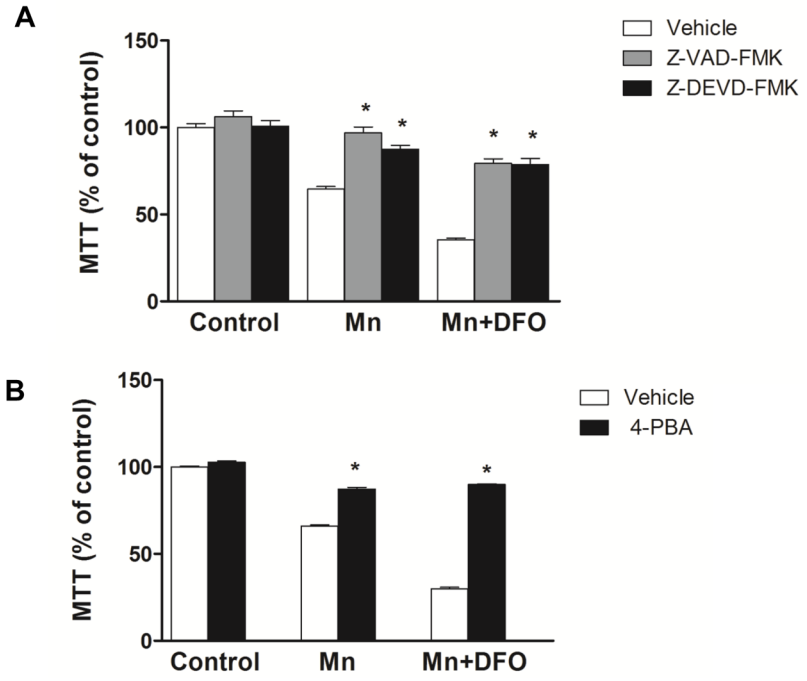

Fig. 6.

Caspase inhibitors or a chemical chaperone prevents Mn-induced neurotoxicity enhanced by iron depletion. (A) Cells were treated with or without DFO, and simultaneously vehicle (white bar), pan-caspase inhibitor Z-VAD-FMK (gray bar, 50μM), or caspase-3 inhibitor Z-DEAD-FMK (black bar, 50μM). Cells were then treated with $MnCl_2$ for 48 h and then cell viability was measured using MTT assay. Data represent mean ± SEM as percent of values observed in vehicle-treated cells (% of control, n = 4–5 samples/treatment). * $P < 0.05$ *vs.* vehicle; two-way ANOVA. (B) Cells were pretreated with vehicle (white bar) or 4-PBA (black bar, 1 mM) and then treated with or without 50 μM DFO. Cells were then treated with $MnCl_2$ for 48 h and then cell viability was measured using MTT assay. Data represent mean ± SEM as percent of values observed in vehicle-treated cells (% of control, n = 4–5 samples/treatment). * $P < 0.05$ *vs.* vehicle; two-way ANOVA.